2017 American Control Conference
Sheraton Seattle Hotel
May 24–26, 2017, Seattle, USA

Nonlinear Model Predictive Air Path Control for Turbocharged SI Engines with Low Pressure EGR and a Continuous Surge Valve

Qilun Zhu, Rohit Koli, Lujia Feng, Simona Onori, *Senior Member, IEEE* and Robert Prucka

***Abstract*—This paper proposes a model predictive strategy for air path control turbocharged Spark Ignition (SI) engines with low pressure Exhaust Gas Recirculation (EGR). The proposed Nonlinear Model Predictive Controller (NMPC) is designed to track manifold pressure and EGR concentration reference, by manipulating throttle, EGR valve, continuous surge valve and waste gate. The NMPC is solved in real time using Sequential Quadratic Programming (SQP) to obtain the desired control actions. Simulation results demonstrate that the proposed model predictive air path control can coordinate all the actuators to track manifold absolute pressure (MAP) and EGR concentration demand with minimal response time.**

I. Introduction

Due to increased stringent fuel economy standards, downsizing and turbocharging of passenger car engines with external Exhaust Gas Recirculation (EGR) has been widely adopted by automotive industry. Both technologies though, significantly increase the complexity of the air path system, challenging the control system design and calibration. Model predictive air path control of turbocharged engines with EGR can coordinate multiple actuators, account for constraints and compensate for system delays. It also requires significantly less calibration effort compared to the conventional feedforward and feedback control strategies. The majority of previous research focuses on the air path control of Compression Ignition (CI) engines with external EGR [1],[2],[3],[4]. Compared to Spark Ignition (SI) engines, CI engines can rely on fast manipulation of air-to-fuel ratio to change torque output, leading to less stringent requirements on air path control. Linear Parameter Varying (LPV) MPC based on heavily simplified air path models are applied in most previous research. Short horizon diesel air path control strategies using explicit MPC were proposed by [3],[4]. Although explicit MPC enables fixed computation time without solving optimization problems iteratively, its high memory demand limits the preview horizon length and significantly reduces its performance in terms of decreasing turbo lag and EGR delay.

Long preview horizons for engine torque can now be used for control due to the development of 'forward-looking' autonomous vehicle technologies, and availability of faster ECUs that enable the computation of iterative optimization algorithms. Long horizon air path LPV MPC methods (e.g. [1]) are based on CI engines and neglect important dynamics like turbocharger surge valve, waste gate, EGR transport delay and compressor surge. This research focuses on long horizon Nonlinear MPC (NMPC) air path control for SI engines with Low Pressure (LP) EGR.

Q. Zhu, R. Koli, L. Feng, S. Onori and R. Prucka are with the Clemson University-International Center for Automotive Research, Greenville, SC, 29607, USA. (Corresponding author, Email: qilun@g.clemson.edu; Phone: 864-283-7220, Fax: 864-283-7208).

The majority of the air path models used in this research have been previously described in various research articles [5][6][7][8]. Extensive research has been done to develop mean-value models for the turbocharger which can be utilized in control oriented air-path models, e.g. [9],[11],[12]. In Low Pressure EGR (LP-EGR) systems, the exhaust extraction is done downstream of the turbine and delivery is done upstream of the compressor. This method allows more exhaust mass to expand through the turbine compared to High Pressure (HP) EGR system, where the EGR loop resides between the exhaust and intake manifold. However, LP-EGR systems have characteristic gas transport delays which are significantly longer than HP-EGR systems. These delays affect transient control of external EGR at the cylinders drastically [13][14]. Previous CI engine control oriented model research approximates the EGR transport delay with lumped volume filling dynamics. The error of this approach may be acceptable for diesel engines since the process of compression ignition has high tolerant to intermittently high EGR dilution [15]. However, inaccurate EGR control can immediately cause misfire or knock for SI engines. This research employs a segmented model to capture EGR transport delays caused by the pipe-like boost volume using a finite element approach. The improved EGR flow modeling accuracy enables MPC to control EGR concentration in the intake manifold accurately with minimal response time.

Nonlinear Programming (NLP) problems are often formulated to solve for the optimal control actions for engine air path systems for each control update, accounting for nonlinearities in system dynamics, objective function and constraints. The NLP may have multiple local optimal solutions. Global NLP solvers, like dynamic programming and particle swarm, can be employed for MPC applications [16],[17]. Stability of MPC with global optimal solutions using terminal state penalties was shown in [18],[19]. However, these global NLP solvers require numerous evaluations of the system model, which are not feasible for engine control applications with fast update frequencies. To reduce model predictive control computational demand sub-optimal strategies are generally used for engine applications [20],[21],[22]. LPV MPC is a widely adopted as a sub-optimal predictive controller [23],[24]. The validity of LPV MPC is based upon the assumption that the system behavior remains linear-like if the system states are not far from the nominal linearization point. The performance of these LPV MPC need to be evaluated against the original NMPC in terms of optimality, constraints violation and closed-loop stability.

Sequential Quadratic Programming (SQP) is a continuous NLP algorithm based on Newton's method [25]. Previous research has discussed the possibility of applying SQP to NMPC [22][26]. The most important advantage of SQP is that it transforms complex NLP into a sequence of sub-level

quadratic programming (QP) problems. The sub-QP can be solved efficiently with algorithms based on active set methods. As a result, the original nonlinear objective and constraint functions are only evaluated before the sub-QP (to compute the Hessian and Jacobian of the NLP problem), saving significant computation time compared to other NLP solvers.

This paper is organized as follows. Section II introduces the control oriented engine air path model. Section III formulates the NLP that solves for desired control actions. Section IV describes the proposed SQP MPC strategy. Simulation results are then analyzed in Section V. Finally, Section VI summarizes the contribution of this research work.

II. Control Oriented Air Path Model

A modular approach is adopted for air path modeling. The individual components of the air path have been modeled separately and then combined together to form the control oriented air path model depicted in Figure 1. $P, T, m, \dot{m}, \omega$, and V are pressure, temperature, mass, mass flow rate, rotational speed and volume respectively. Subscriptions $1, 2, 3, 4, E, B, W, T, Comp, Turb,$ and exh are the intake manifold, exhaust manifold, ambient, boost volume (between compressor and throttle), EGR, compressor recirculation valve (or surge valve), turbine bypass valve (or waste gate), intake throttle, compressor, turbine and post-turbine exhaust respectively.

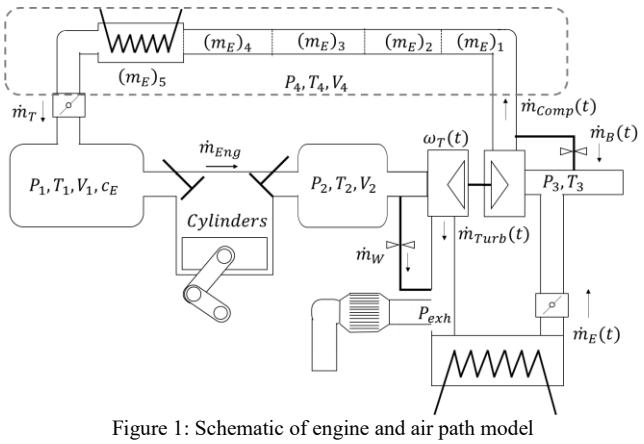

Figure 1: Schematic of engine and air path model

A. Gas transport dynamics in boost volume

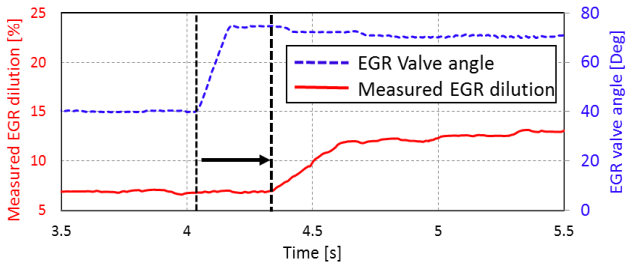

Figure 2: Step response of oxygen sensor based EGR measurement installed at compressor outlet location

The boost volume, V_4, has been traditionally considered as a lumped volume in the turbocharged diesel engine air path [7][8][9]. However, its long thin pipe-like geometry results in negligible mixing between EGR and air species. Experimental testing has confirmed this phenomenon, as shown in Figure 2, where a step input in EGR valve position results in a transport time delay and mixing response from the EGR measurement sensor installed at the throttle valve. The mixing response is primarily due to the manifold filling and emptying dynamics. These results suggest that the lumped volume assumption can result in inaccurate EGR concentration estimation and control.

Transport delay models are also not suitable for the control-oriented pipe flow computation because they have an infinite system order. Although it can be approximated by a Páde method, a fixed transport time is required. In the boost volume case the transport time changes rapidly according to the throttle and compressor mass flow. *Nowak et al.* [28] concluded that the pipe flow can be modelled by a parabolic differential equation (PDE) with respect of both time and pipe length. Discretization of both time and pipe length is required to solve this PDE. Therefore, this research separates the pipe into n_i segments. Each segment has a smaller length to radius ratio than complete pipe, making it possible to be approximated by lumped volume model. For the i^{th}segment, conservation of EGR mass $(m_E)_i$ leads to:

$$(\dot{m}_E)_i = (\dot{m}_{EGR_{in}})_i - (\dot{m}_{EGR_{Out}})_i \quad (1)$$

$$(\dot{m}_{EGR_{Out}})_i = \frac{(m_E)_i R T_4}{P_4 V_4} (\dot{m}_{out})_i \quad (2)$$

where:

$$(\dot{m}_{out})_i = \frac{\dot{m}_T - \dot{m}_{Comp}}{n_i} i;$$

$$(\dot{m}_{EGR_{in}})_i = (\dot{m}_{EGR_{Out}})_{i-1};$$

R is ideal gas constant.

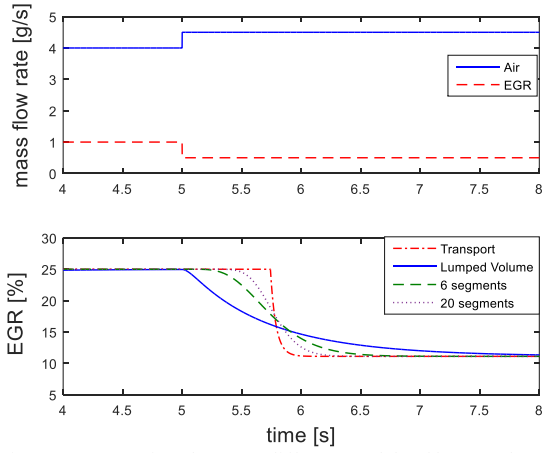

Figure 3: Comparison between different models of boost volume.

Figure 3 compares different models of the boost volume. The simulation describes a situation where EGR concentration decreases at 5s while the total flow rate is fixed. In this case, the pipe flow can be modelled by a transport delay, serving as a benchmark. It can be observed that the segmented approach generates a more accurate estimation of the intake manifold EGR percentage as compared to the lumped volume method. A higher number

of segments results in better accuracy, but results in higher system order. A 10 segments transport delay model was chosen for this research.

Remark: The increased system order from the segmented pipe model does not increase the computation load of real time NLP that solves the NMPC. The decision variables of the NLP remain the same since they are still the control actions of the preview horizon. However, the higher system order increases the computational load of state estimation, which is outside of the scope of this research.

B. Turbocharger model

The turbocharger model computes the air mass flow through the turbine and compressor according to pressure differential (between the inlet and outlet of both turbine and compressor) and turbo speed. In general, the turbocharger model takes the form as the following:

$$\dot{\omega}_T = f_T(\omega_T, P_2, P_e, P_3, P_4, T_3, T_e) \tag{3}$$

$$\left[\dot{m}_{Turb}, \dot{m}_{Comp}, T_{Comp}\right]^T = g_T(\omega_T, P_2, P_e, P_3, P_4, T_3, T_e) \tag{4}$$

Equation (3) can be derived from Newton's second law:

$$\dot{\omega}_{Turbo} I_{Turbo} = \tau_{Turb} - \tau_{Comp} + \tau_{Friction} \tag{5}$$

$$\tau_{Comp} = \dot{m}_{Comp}.c_p.T_3\left[\left(\frac{P_2}{P_3}\right)^{\frac{K-1}{K}} - 1\right].\left[\frac{1}{\eta_{Comp}.\omega_T}\right] \tag{6}$$

$$\tau_{Turb} = \dot{m}_{Turb}.c_{p_e}.T_e\left[1 - \left(\frac{P_2}{P_e}\right)^{\frac{K_e-1}{K_e}}\right].\left[\frac{\eta_{Turb}}{\omega_T}\right] \tag{7}$$

where:

I_{Turbo} is the inertia of the turbocharger rotor;

$\tau_{Friction}$ is the friction torque;

c_p and c_{pe} are the constant pressure heat capacity of ambient air and exhaust;

K and K_e are the heat capacity ratio of ambient air and exhaust;

η_{comp} and η_{Turb} are efficiency of compressor and turbine.

The air mass flow and efficiency of the compressor and turbine can be computed from ω_T, P_2, P_e, P_3 and P_4 using lookup tables (commonly referred to as turbo 'maps'). A majority of compressor maps exhibit a nearly linear surge limit with respect to pressure ratio and mass flow rate [27]. The mass flow rate at which surge occurs can be explicitly modeled as a linear function of pressure ratio:

$$\dot{m}_{Surge} = c_1\frac{P_2}{P_A} + c_2 \tag{8}$$

where c_1 and c_2 are coefficients fitted to the manufacturers map.

Define ζ as:

$$\zeta = \dot{m}_{Comp} - \dot{m}_{Surge} \tag{9}$$

Surge occurs when $\zeta \leq 0$.

C. Engine air mass flow and control volume pressure

The engine mass flow has been modeled using the widely used 'speed-density' approach [29] as the following:

$$\dot{m}_{Eng} = \frac{P_1}{RT_1}\frac{\eta_V V_d \omega_{Eng}}{4\pi} \tag{10}$$

where η_V is volumetric efficiency, ω_{Eng} is engine speed, and V_d is engine displacement volume.

The exhaust mass flow has been assumed to be the same as the engine mass flow. This assumption is under the consideration that the pressure dynamics in the exhaust manifold are not significantly affected by the additional fuel mass flow rate. The exhaust temperature has been modeled empirically as a function of engine speed and load:

$$T_2 = f_{T2}\left(\dot{m}_{Eng}, \omega_{Eng}\right) \tag{11}$$

f_{T2} is a two dimensional lookup table derived from a full factorial design of experiments executed in a 1-D engine simulation software.

The intake manifold pressure dynamics can be derived from the ideal gas law and mass balance:

$$\dot{P}_2 = \frac{RT}{V_m}\left(\dot{m}_T - \dot{m}_{Eng}\right) \tag{12}$$

The exhaust manifold and boost volume pressures are modelled similar to the intake manifold. Finally, the complete nonlinear air path model in state space form is given below:

$$\begin{aligned} \dot{x} &= f_x(x,u) \\ y &= f_y(x) \\ z &= f_z(x) \end{aligned} \tag{13}$$

where:

$x \in \mathbb{R}^{10}, x = [P_1, P_2, P_4, \omega_T, m_{EGR}, (\dot{m}_e)_i]^T, i = 1,2, \ldots 10;$

$u \in \mathbb{R}^4, u = [\dot{m}_T, \dot{m}_W, \dot{m}_B, \dot{m}_{EGR}]^T;$

$y \in \mathbb{R}^2, y = [P_1, c_{EGR}]^T;$

$z \in \mathbb{R}^2, z = [P_1 - P_4, \zeta]^T;$

m_{EGR} is the EGR mass in the intake manifold;

c_{EGR} is the EGR concentration in the intake manifold;

$P_1 - P_4$ is the constraint to ensure feasible non-negative throttle air mass flow.

For the model (13) to be used in the NMPC formulation, nodes discretization must be implemented. Conventionally, an Euler approach can discretize the nonlinear model directly. With sampling time Δt, the discrete state transition function is computed as:

$$x(k+1) = x(k) + f_x(x,u)\Delta t \tag{14}$$

The air path dynamics become very fast at high engine speed. In order to maintain numerical stability, the Euler approach requires very fast sampling time to capture the filling dynamics of small volumes, like boost volume V_4 and exhaust manifold V_2. This short sampling time may not be sufficient to complete the NMPC computation. One solution

is to eliminate the fast dynamics for the given sampling time as to allow for the NMPC to terminate its computation. However, this results in reduced model accuracy and a varying order system, which is not favorable for NMPC formulation. In order to solve this dilemma, this research applies a State Transition Matrix (STM) approach for model discretization. After linearizing the model at the nominal operating points, the discrete state transition function can be computed as:

$$x(k+1) = f_{xd}\big(x(k+1), u(k)\big) = e^{A\Delta t}x(k) + \int_0^{\Delta t} e^{A\tau}d\tau\, Bu(k) \tag{15}$$

where A and B are state space matrices from the linearized model.

From equation (15), the STM methods finds the exact solution of the linearized continuous system over the sampling period Δt. It preserves the system stability information while maintaining system order regardless of the length of Δt. However, the integral term in equation (15) grows exponentially if the system is unstable. In this case, an excessive large Δt can still result in numerical issues. Table I compares Euler and STM approaches in terms of the maximum sampling, which results in numerical stability issues. It can be concluded that the STM approach allows for much slower NMPC update frequency even with high engine speed than the Euler method.

TABLE I: COMPARISON OF MAXIMUM SAMPLING TIME BETWEEN EULER AND STM APPROACHES.

Engine speed	Max Δt: Euler	Max Δt: STM
2000 RPM	50 ms	220 ms
6000 RPM	15 ms	75 ms

Remark: The STM approach completes both system linearization and discretization at the same time. Considering system linearization is inevitable for most NMPC applications, the STM method does not increase the computational load significantly.

III. OPTIMIZATION PROBLEM FORMULATION

The objective of the proposed model predictive air path controller is to track MAP and EGR concentration of the intake manifold. Therefore, the stage cost of the objective function should penalize the least square reference tracking error and control effort. After adding a terminal state penalty for stability consideration the objective function of the NMPC is:

$$J_0\big(x(k), U(k)\big) = x(k+N)^T Q_f x(k+N) + \sum_{i=k}^{k+N-1} \frac{1}{2} q\left(y(i) - y_{ref}(i)\right)^2 + u(i)^T r u(i) \tag{16}$$

where:

$r \in \mathbb{R}^{4\times4}_{>0}, q \in \mathbb{R}^{2\times2}_{>0}, Q_f \in \mathbb{R}^{10\times10}_{>0}$

$U(k) = [u(k), u(k+1), \dots u(k+N-1)]^T$.

The penalty on terminal states is not sufficient to guarantee the stability of sub-optimal MPC. This issue will be addressed later in this document. The objective function of this specific control application has a least-square-like structure that favors Gauss-Newton methods. The next section discusses exploiting this property to reduce computation load.

The proposed controller requires $\zeta \le 0$ to avoid compressor surge. The air mass flow through all the control valves is required to be non-negative, and the upstream pressure must be higher than the downstream pressure so that the valve flow rate is physically feasible. Finally, the following equation shows the complete NLP that is solved in every NMPC update to obtain the optimal control sequence for all N steps of the future horizon.

$$\min_{U(k)} J_0\big(x(k), U(k)\big) \quad \text{s.t.} \quad \begin{cases} x(i+1) = f_{xd}\big(x(i), u(i)\big), \\ y(i) = f_y\big(x(i)\big), \\ z(i) = f_z\big(x(i)\big), \\ z(i) \le 0, \\ -u(i) \le 0. \end{cases} \tag{17}$$

where $i = k, k+1, \dots k+N-1$.

The equality constraints of system dynamics can be transferred to the objective function, leading to a new objective function $J\big(x(k), U(k)\big)$. The new NLP problem only has inequality constraints, and can be written in a more compact form:

$$\min_{U(k)} J\big(x(k), U(k)\big) \quad \text{s.t.} \quad l\big(x(k), U(k)\big) \le \mathbf{0}. \tag{18}$$

where l: $\mathbb{R}^{4N} \to \mathbb{R}^{(2+4)N}$.

IV. SQP STRATEGY WITH GAUSSIAN HESSIAN APPROXIMATION

This research utilizes the SQP algorithm proposed by [26] to solve the optimization problem (18) during each MPC sampling time. The following section briefly introduces the SQP algorithm. With a given initial guess of U (represented by U_0), the SQP computes the searching direction ΔU by solving a sub-quadratic programing problem as follows:

$$\min_{\Delta U(j)} \frac{1}{2}\Delta U^T H J_{(x_k, U_0)} \Delta U + \Delta U^T \nabla J_{(x_k, U_0)} \quad \text{s.t.} \quad l_{(x_k, U_0)} + \nabla l_{(x_k, U_0)} \Delta U \le \mathbf{0} \tag{19}$$

where $HJ_{(x_k, U_0)}$ is the Hessian at (x_0, U_0), and $\nabla J_{(x_k, U_0)}$ is the Jacobian at (x_0, U_0).

The search step size toward direction ΔU is scaled by a factor α, which was generated by solving a line search problem of a merit function of the original NLP:

$$\alpha(i) = arg\min_{\alpha} g(U + \alpha\Delta U) \tag{20}$$

where

$$g(U) = J(x(k), U) + \sigma \sum_{i=1}^{q} \max\left(0, l_i(x(k), U)\right) \tag{21}$$

q is the total number of constraints, and σ is the penalty on the constraints violation.

For each major iteration j (whereas the iterations solving the sub-QP problems are referred to as minor iterations), the updated solution is calculated as:

$$U^* = U_0(j+1) = U_0(j) + \alpha\Delta U(j) \tag{22}$$

The $U_0(j+1)$ is the starting point of the next major iteration. The SQP is considered as converged if the search step, $\alpha\Delta U(j)$, is smaller than a certain threshold. In this situation, the algorithm terminates, outputting U^* as the final solution.

V. Simulation Results

Figure 4 and Figure 5 show the performance and control actuation of the proposed SQP model predictive air path controller in simulation. The MPC has a sampling time of 50 ms and 10 steps preview/control horizon. The simulated scenario includes a "tip-in" and a "tip-out" maneuver while the engine speed is fixed at both 2000 RPM and 6000 RPM.

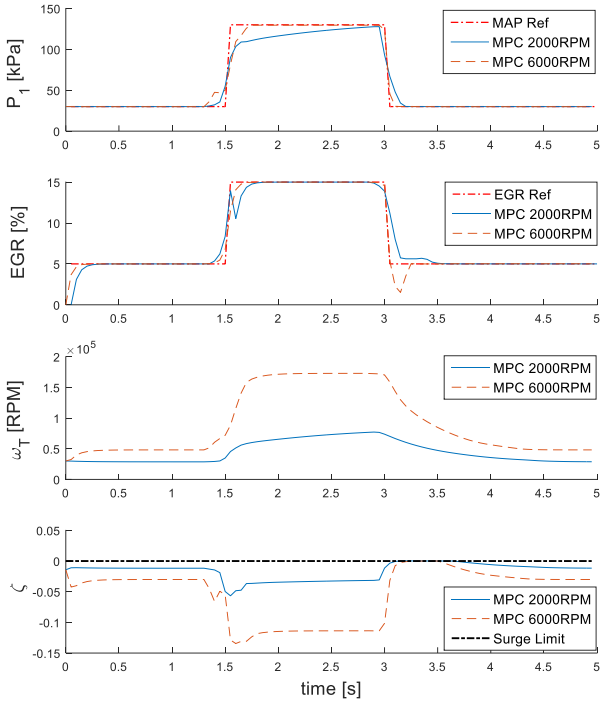

Figure 4: Performance of the proposed model predictive engine air path control during "tip-in" and "tip-out" situations.

Figure 4 shows that the proposed model predictive air path controller successfully tracks MAP and EGR references during both tip-in and tip-out situations without violating the surge constraint (and other constraints described previously). Before tip-in, the NMPC closes the waste gate ahead of time to increase turbo speed and boost pressure. At the instance of tip-in, the throttle is opened to an overshooting position, increasing the intake manifold pressure rapidly. It is observed that the NMPC opens surge valve initially to allow air mass flow into the boost volume (negative surge valve flow) while its pressure is less than the ambient. EGR valve shows overshooting behaviors to compensate for manifold filling delay. Furthermore, the NMPC foresees the transport delay caused by the pipe between compressor and throttle, which is modelled as a segmented pipe as discussed previously. Therefore, the EGR valve opens earlier than the tip-in action.

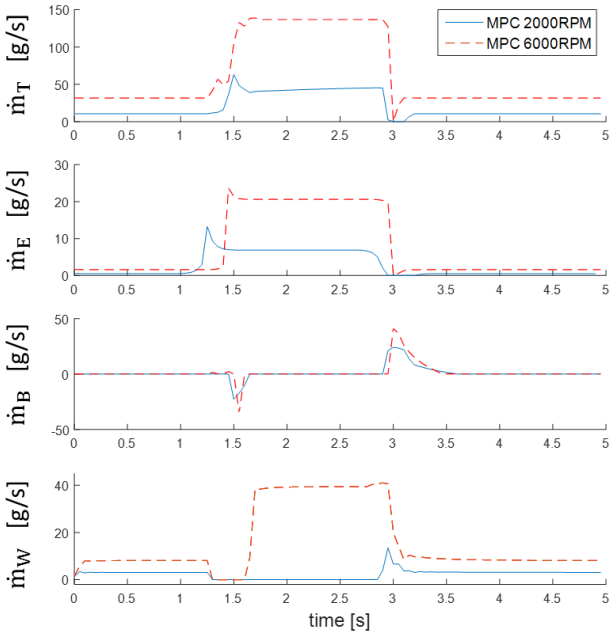

Figure 5: Control actions of the proposed model predictive engine air path control during tip-in and tip-out situations.

During the tip-out, the throttle is fully closed ahead of time to compensate for the non-negative throttle air mass flow constraint and intake manifold emptying dynamics. The throttle re-opens when the intake manifold drops to the desired target. The EGR valve shows similar maneuvers as the throttle to compensate for constraints and intake manifold delay with more lead action considering the EGR transport delay. The waste-gate is opened at the instance of tip-out to reduce turbo speed. In the meantime, the surge valve is also opened to reduce boost volume pressure quickly to avoid compressor surge. These actions can also be observed from current production turbocharged engine control strategies. After increasing the engine speed from 2000 to 6000 RPM, the air mass flow through the entire air path increases significantly. As a result, the NMPC reduces valve overshoot and lead-time to account for the faster system dynamics.

VI. Conclusion

This research proposes a nonlinear model predictive control strategy for air path control of turbocharged SI engines with LP-EGR. The control objective is to track intake manifold MAP and EGR concentration references

while minimizing control effort. This NMPC also respects compressor surge and actuator saturation constraints during the search for optimal control actions. A SQP algorithm is tailored for this NMPC application to improve the computational efficiency. It exploits the least-square like structure of the NLP formulated for MPC to simplify computation of the Hessian matrix. The merit function step scaling improves global convergence performance and eliminates steady state control chattering issues. Finally, the STM discretization method enables sufficient sampling time for the computation of NMPC considering the accelerated air path dynamics during high engine speed operation. Simulation results demonstrate that the proposed model predictive air path control strategy achieves its design objectives, in terms of tracking MAP and EGR concentration reference, minimizing control actuation and respecting compressor surge constraints. The computational time analysis of the proposed SQP MPC demonstrates high potential for real-time implementation with current prototype controllers or future production ECUs.

ACKNOWLEDGEMENT

The authors gratefully thank FCA US LLC for helpful discussions and financial support of this research project.

REFERENCES

[1] H.J. Ferreau, P. Ortner, P. Langthaaler, L. del Re, and M. Diehl, "Predictive control of a real-world diesel engine using an extended online active set strategy", *Annual Reviews in Control*, vol. 31, no. 2, pp.293-301, 2007.

[2] M. Herceg, T. Raff, R. Findeisen, and F. Allgöwer, "Nonlinear model predictive control of a turbo-charged diesel engine", *in Proc. of IEEE International Conference on Control Applications*, pp. 2766-2771, Oct., 2006, Munich, Germany.

[3] P. Ortner, P. Langthaler, J. Ortiz, L. del Re, "MPC for a diesel engine air path using an explicit approach for constraint systems", *in Proc. of 2006 IEEE International Conference on Control Applications*, pp. 2760-2765, Munich, Germany, Oct., 4-6, 2006.

[4] M. Huang, K. Zaseck, K. Butts and I. Kolmanovsky, "Rate-based model predictive controller for diesel engine air path: design and experimental evaluation", *IEEE Transactions on Control Systems Technology*, vol. PP, no. 99, pp. 1-14, 2016.

[5] Y. Nishio, M. Hasegawa, K. Tsutsumi, J. Goto and et al. "Model Based Control for Dual EGR System with Intake Throttle in New Generation 1.6L Diesel Engine," *SAE Technical Paper,* 2013-24-0133, 2013.

[6] O. Grondin, "Control of a Turbocharged Diesel Engine Fitted with High Pressure and Low Pressure Exhaust Gas Recirculation Systems," *IEEE Conference on Decision and Control, 28th Chinese Control Conference*, Shanghai, P.R. China, December 16-18, 2009

[7] J. Wang, "Air fraction estimation for multiple combustion mode diesel engines with dual-loop EGR systems" *Journal of control engineering practice Control Engineering Practice*, vol. 16, no. 12, pp. 1479– 1486, 2008

[8] F. Castillo, "Simultaneous Air Fraction and Low-Pressure EGR Mass Flow Rate Estimation for Diesel Engines," *5th Symposium on System Structure and Control Part of 2013 IFAC Joint Conference SSSC Grenoble*, France, February 4-6, 2013

[9] J. Jensen, A. Kristensen, S. Sorenson, N. Houbak and et al. "Mean Value Modeling of a Small Turbocharged Diesel Engine," *SAE Technical Paper,* no. 910070, 1991.

[10] L. Eriksson, "Modeling and Control of Turbocharged SI and DI Engines", *Oil & Gas Science and Technology – Rev. IFP*, vol. 62, no. 4, pp. 523-538, 2007.

[11] O. Leufven, L., Eriksson, "Surge and Choke Capable Compressor Model", *in Proc. of the 18th World Congress, The International Federation of Automatic Control*, Milano, Italy, August 28 - September 2, 2011

[12] J. El Hadef, G. Colin, Y. Chamaillard and V. Talon, "Physical-Based Algorithms for Interpolation and Extrapolation of Turbocharger Data Maps," *SAE Int. J. Engines,* vol. 5, no. 2, 2012.

[13] R. Koli, K. Siokos, R.Prucka, S. Jade and et al. "A Control Algorithm for Low Pressure - EGR Systems Using a Smith Predictor with Intake Oxygen Sensor Feedback," *SAE Technical Paper*, no. 2016-01-0612, 2016.

[14] F. Liu and J. Pfeiffer, "Estimation Algorithms for Low Pressure Cooled EGR in Spark-Ignition Engines," *SAE Int. J. Engines*, vol. 8, no. 4, 2015.

[15] M. Zheng, "Diesel engine exhaust gas recirculation – a review on advanced and novel concepts", *Journal of Energy Conversion and Management*, vol. 45, no. 6, pp. 883–900, 2004.

[16] M. Diehl, "Robust dynamic programming for min-max model predictive control of constrained uncertain systems", *IEEE Transactions on Automatic Control*, vol. 49, no. 12, pp. 2253-2257, Dec., 2004.

[17] E.S. Meadows, "Dynamic programming and model predictive control", *in Proc. of 1997 American Control Conference*, pp. 1635-1639, Jun., 1997, Albuquerque, USA.

[18] J.B. Rawlings and D.Q. Mayne, *Model Predictive Control: Theory and Design*, Nob Hill Publishing, Madison, WI, 2009.

[19] D.Q. Mayne, J.B., Rawlings, C.V. Rao and P.O.M. Scokaert, "Constrained model predictive control: Stability and optimality", *Automatica*, vol. 36, no. 6, pp. 789~814, 2000.

[20] T. Ohtsuka, "A continuation/GMRES method for fast computation of nonlinear receding horizon control", *Automatica*, vol. 40, no. 4, pp. 563~574, 2004.

[21] M. Lazar, "Flexible Control Lyapunov Functions", *in Proc. of 2009 American Control Conference*, pp. 102~107, Jun. 2009, St. Louis, USA.

[22] R. Quirynen, B. Houska, M. Vallerio, D. Telen, F. Logist, J. Van Impe and M. Diehl, "Symmetric algorithmic differentiation based exact Hessian SQP method and software for Economic MPC", *in Proc. of 2014 IEEE 53rd Annual Conference on Decision and Control*, pp. 2752~2757, 2014.

[23] Q. Zhu, S. Onori and R. Prucka, "Pattern recognition technique based active set QP strategy applied to MPC for a driving cycle test", *in Proc. of 2015 American Control Conference*, pp. 4935~4940. Jul., 2015, Chicago, USA.

[24] Sharma, R., Nešic, D. and Manzie, C. "Idle speed control using linear time varying model predictive control and discrete time approximations", *in Proc. of 210 IEEE International Conference on Control Applications*, pp. 1140-1145, Yokohama, Japan, Sep., 2010.

[25] D.P. Bertsekas, *Nonlinear Programming*, 2nd Ed. 1999, Athena Scientific, pp. 431~448.

[26] Q. Zhu, S. Onori and R. Prucka, "Nonlinear economic model predictive control for SI engines based on sequential quadratic programming", *in Proc. of 2016 American Control Conference*, Jul., 2016, Boston, USA.

[27] K. Bruhn, "Application guidelines for centrifugal surge control systems", *Gas Machinery Research Council Southwest Research Institute,* April 2008

[28] U. Nowak, J. Frauhammer and U. Nieken, "A fully adaptive algorithm for parabolic partial differential equations in one space dimension", *Computers chem. Engng*, vol. 20, no. 5, pp. 547-561, 1996.

[29] L. Guzzella and C.H. Onder, *Introduction to modeling and control of internal combustion engine systems*, 2nd ed., Springer, 2009.

[30] S.P. Han, "A globally convergent method for nonlinear programming", *J. Optimization Theory and Applications*, vol. 22, no. 3, pp. 297, 1977.